118 Basilar Artery Trunk Aneurysm: Spontaneous Subarachnoid Hemorrhage due to an Aneurysm Associated with a Fenestration of the Basilar Artery, Endovascular Coil Occlusion

Muhammad AlMatter, Marta Aguilar Pérez, Oliver Ganslandt, and Hans Henkes

Abstract

The following case concerns a young female patient with spontaneous subarachnoid hemorrhage (SAH) due to a ruptured aneurysm originating at a non-fused, fenestrated proximal segment of the basilar artery. The aneurysm was treated with endovascular coil embolization which resulted in complete exclusion, and the patient showed a complete clinical recovery. A second aneurysm originating from the left internal carotid artery (ICA) was diagnosed during the follow-up and was treated in a separate session using a flow diverter stent. Three additional cases of ruptured aneurysms of non-fused basilar arteries are presented at the end of the discussion. Basilar artery fenestration with associated aneurysm formation is the main topic of this chapter.

Keywords

Basilar artery trunk · Fenestration · Subarachnoid hemorrhage · Coiling · pCONUS

Patient

A previously healthy 28-year-old female patient presenting with spontaneous subarachnoid hemorrhage resulting in a severe headache of sudden onset (Hunt and Hess grade I). The physical examination was unremarkable.

Diagnostic Imaging

Due to the sudden onset of the symptoms, a cranial non-contrast computer tomography (NCCT) was performed, which revealed a moderate subarachnoid hemorrhage (SAH) mainly in the prepontine cistern with minor extension into the third, fourth, and the left lateral ventricle (Fisher grade 4). The CT angiography (CTA) revealed a small aneurysm originating from the proximal third of the basilar artery (BA) trunk proximal to the origin of the anterior inferior cerebellar arteries (AICA). The patient was then admitted to the angio-suite for complete cerebral angiography. The digital subtraction angiography (DSA)

M. AlMatter (✉) · M. Aguilar Pérez · H. Henkes
Neuroradiologische Klinik, Klinikum Stuttgart, Stuttgart, Germany
e-mail: muh.almatter@gmail.com; martaaguilarperez@yahoo.es; hhhenkes@aol.com

O. Ganslandt
Neurochirurgische Klinik, Neurozentrum, Klinikum Stuttgart, Stuttgart, Germany
e-mail: o.ganslandt@klinikum-stuttgart.de

H. Henkes et al. (eds.), *The Aneurysm Casebook*,
https://doi.org/10.1007/978-3-319-77827-3_64

confirmed the CTA finding of a 6-mm aneurysm of the BA originating at the beginning of a short segmental non-fusion 1-cm proximal to the origin of the AICAs. The left and the right AICA originated from the left and right non-fused segment, respectively. The DSA also revealed a small aneurysm of the left internal carotid artery (ICA) originating from the dorsal wall just proximal to the posterior communicating artery (PcomA) (Fig. 1).

Treatment Strategy

Due to the distribution of the SAH, the BA trunk aneurysm was presumed to be the most likely cause of the SAH. As the fundus-to-neck ratio was favorable, the decision was made to treat with endovascular coil occlusion. In anticipation of a possible coil dislocation and the emergent need for an adjunctive device (i.e., a stent), the patient was pretreated with dual antiplatelets the evening before the treatment.

Treatment

Procedure #1, 12.06.2014: endovascular coil occlusion of a ruptured aneurysm at the proximal third of the BA trunk

Anesthesia: general anesthesia; intraprocedural medications, 1000 mg thiopental (Trapanal, Nycomed) IV, 1 mg glyceroltrinitrate (Nitrolingual infus., G. Pohl - Boskamp) IA

Premedication: 1× 500 mg ASA (Aspirin, Bayer Vital) and 1× 180 mg ticagrelor (Brilique, AstraZeneca) both PO the evening prior to the endovascular treatment

Access: right common femoral artery; 1× 6F sheath (Terumo); *guide catheter*, 1× 6F Heartrail II (Terumo); *microcatheter*, 1× Echelon-14 (Medtronic); *microguidewire*, 1× Synchro2 0.014″ 200 cm (Stryker)

Coils: 1× GDC 360° 6/11 (Stryker), 1× HydroCoil 5/15, 1× MicroPlex10 4/8; 3× MicroPlex10 3/8; 1× MicroPlex10 2/6 (MicroVention)

Course of treatment: after completing the four-vessel angiography and selecting an appropriate working projection, the guide catheter was advanced into the mid-cervical segment of the left vertebral artery. The microcatheter was then advanced over a 0.014″ guidewire into the sac of the aneurysm. The aneurysm was then completely filled using the aforementioned coils. At the end of the procedure, the microcatheter was then carefully removed from the aneurysm using the microguidewire (Fig. 2).

Duration: 1st–35th DSA run: 105 min; fluoroscopy time: 44 min

Complications: none

Post medication: standard posthemorrhagic vasospasm prophylaxis; ASA and ticagrelor were discontinued

Follow-Up and Subsequent Treatment

The patient had an uneventful recovery after the first endovascular treatment. Although the BA trunk aneurysm was the most likely cause of the hemorrhage, rupture of the left ICA aneurysm could not be completely ruled out. The patient was thus offered and accepted endovascular treatment of the left ICA aneurysm during the same hospitalization. As this was a side-wall wide-necked aneurysm, covering with a flow diverter was deemed to be the most suitable treatment.

Procedure #2, 17.06.2014: endovascular treatment of a wide-necked left ICA aneurysm at the level of the PcomA using flow diversion

Anesthesia: general anesthesia; 5000 U unfractionated heparin IV, 500 mg ASA IV, 600 mg clopidogrel PO, 1 mg glyceroltrinitrate (Nitrolingual infus., G. Pohl - Boskamp) IA

Access: right common femoral artery, 1× 6F sheath (Terumo); *guide catheter*, 1× 6F Heartrail II (Terumo); *microcatheter*, 1× Excelsior XT-27 (Stryker); *microguidewire*, 1× Synchro2 0.014″ (Stryker)

Implant: 1× p64 flow modulation device 3.5/15 mm (phenox)

Course of treatment: the 6F guiding catheter was placed into the cervical segment of the left ICA. The terminal ICA was then catheterized with an Excelsior XT-27 microcatheter through which the aforementioned p64 flow diverter stent (FDS) was inserted and deployed into the PcomA

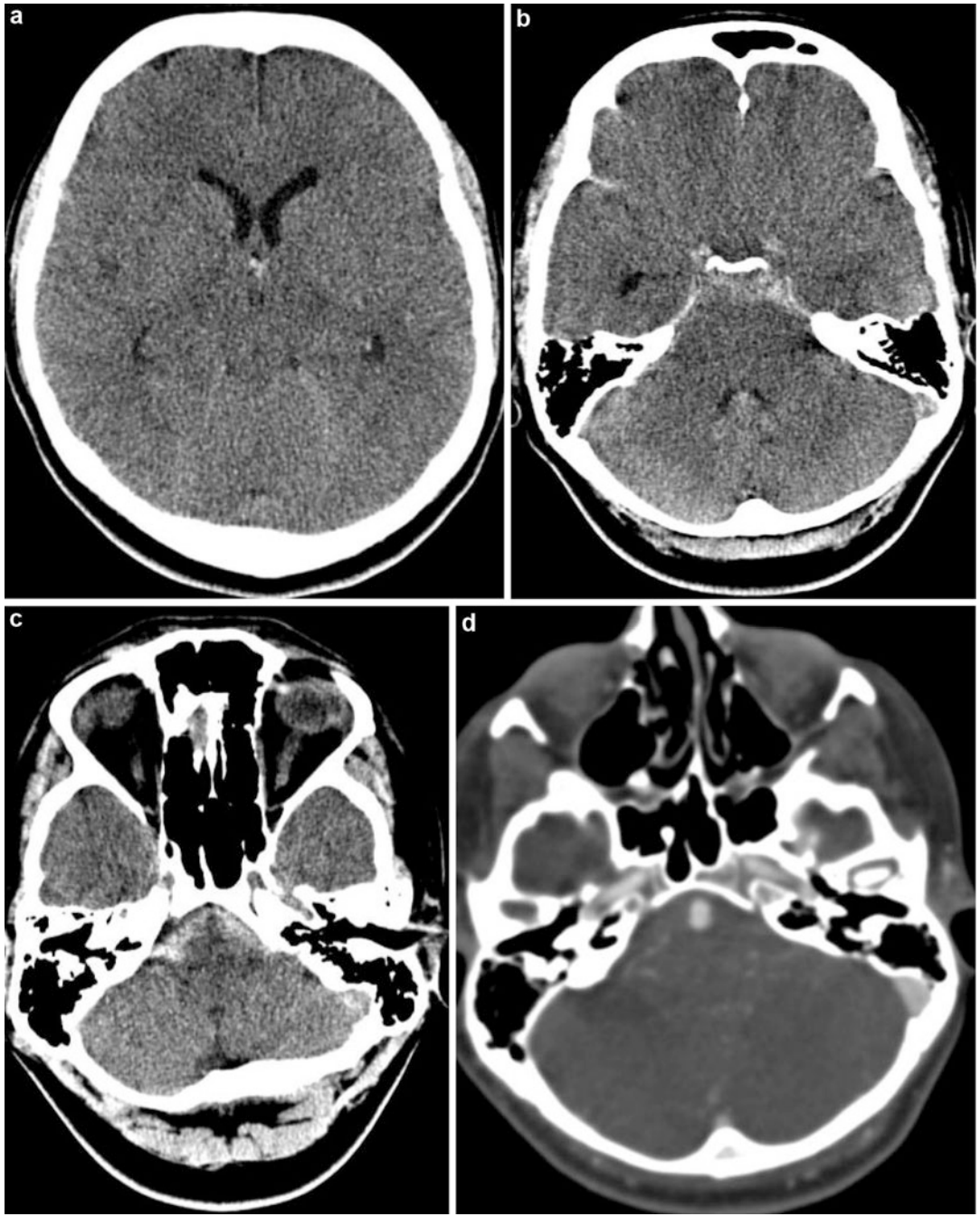

Fig. 1 (continued)

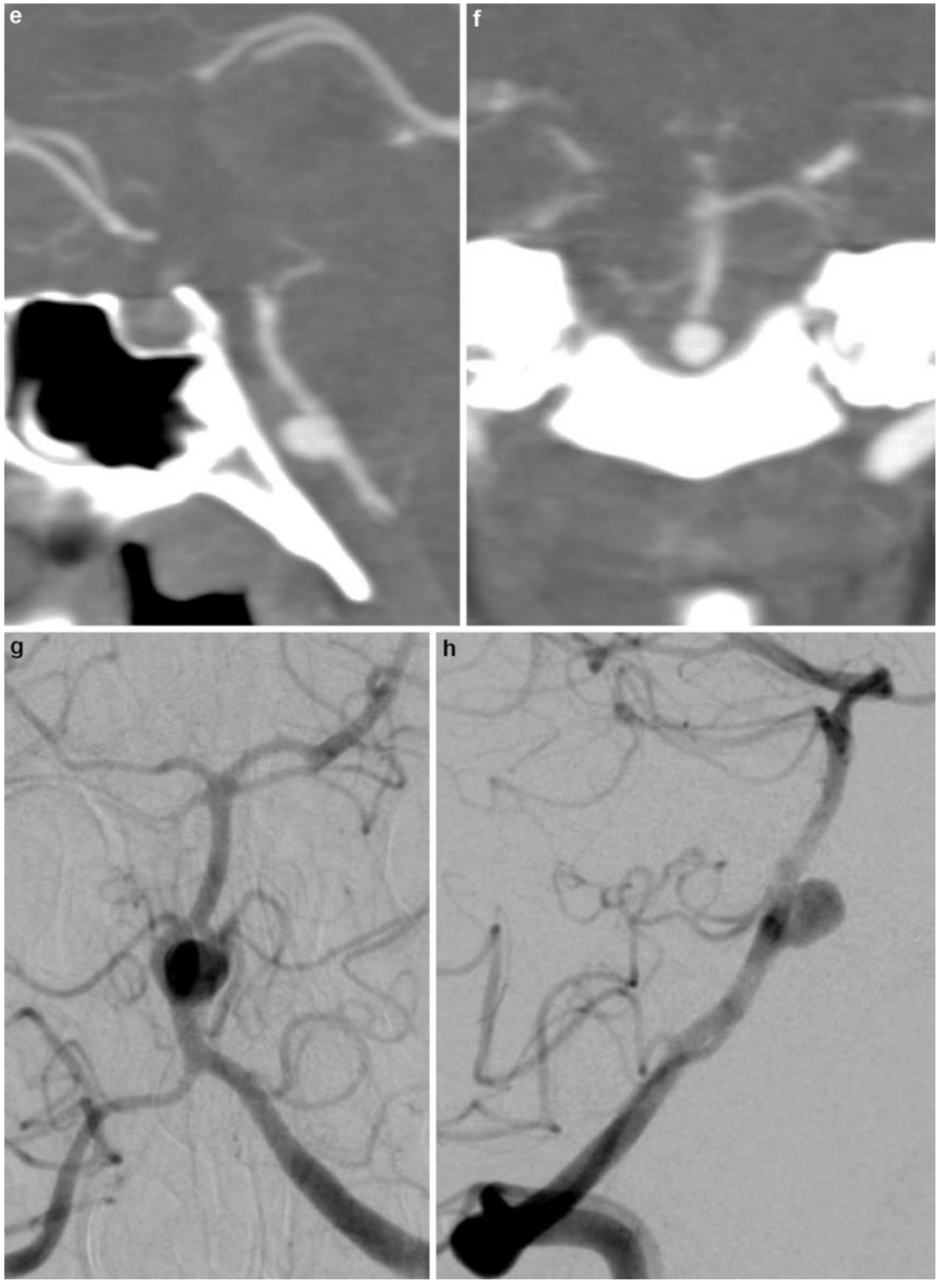

Fig. 1 (continued)

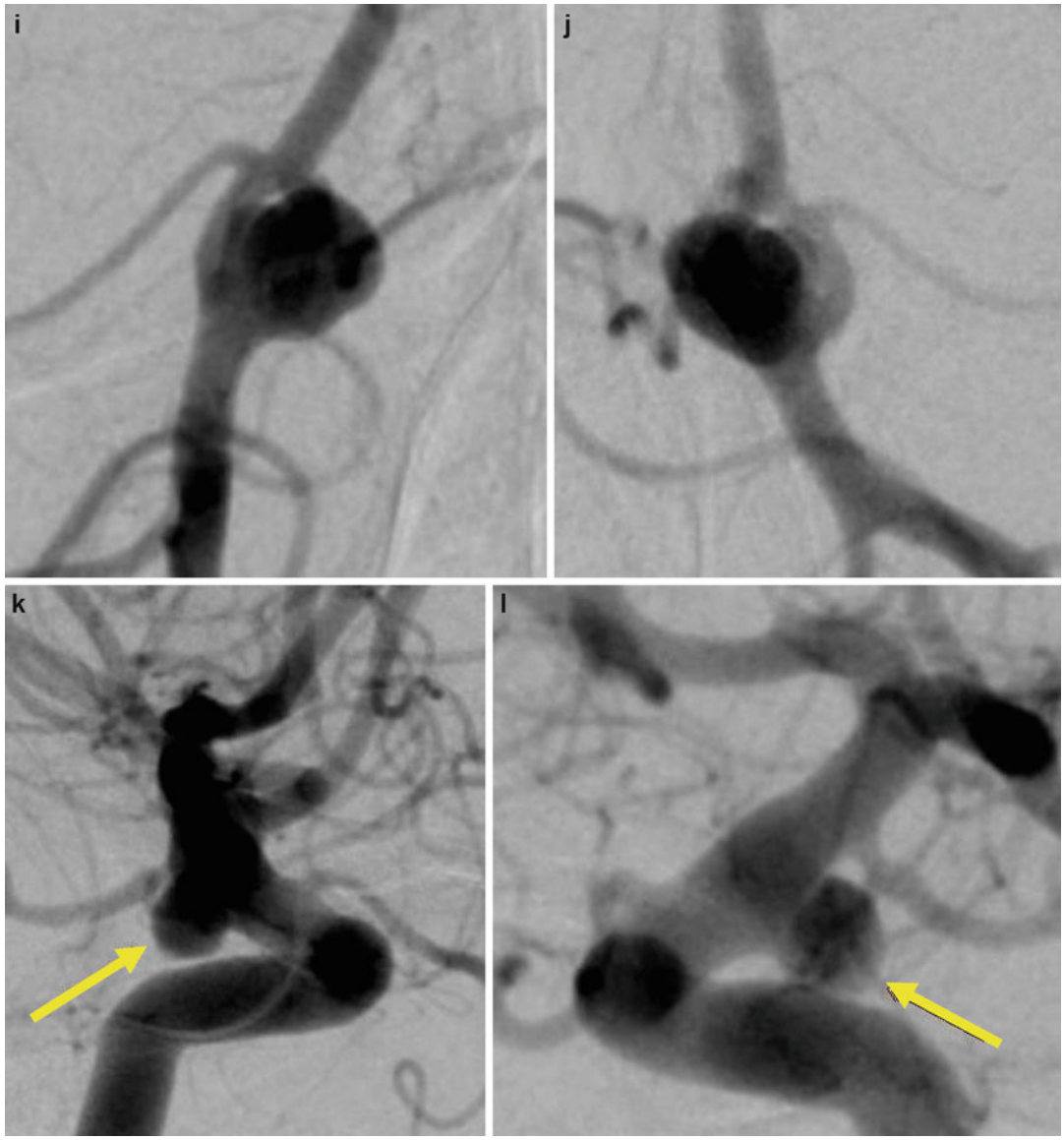

Fig. 1 Diagnostic imaging in a 28-year-old woman presenting with a severe headache of sudden onset. The initial NCCT upon admission showed a moderate subarachnoid hemorrhage with blood in the prepontine cistern (**a**) extending into the fourth (**b**) and the third ventricle (**c**) (Fisher grade 4). Axial (**d**), sagittal (**e**), and coronal (**f**) reformations of the CTA at admission showing a small, anteriorly oriented aneurysm on the proximal third of the basilar artery trunk. DSA in posterior-anterior (**g**), lateral (**h**), and 45° oblique (**i**, **j**) projections after selective injection of the left vertebral artery confirming the CT findings of an aneurysm of the proximal third of the basilar artery trunk, with superior and anterior orientation. The distal portion of the proximal third of the basilar artery is not fused ("fenestrated") and the aneurysm originates at the point of non-fusion. Note also that both AICAs originate from a non-fused BA segment. Lateral (**k**) and oblique (**l**) views of the selectively injected left ICA showing a wide-necked side wall aneurysm of the left ICA with a diameter of 3.5 mm just proximal to the origin of the PcomA

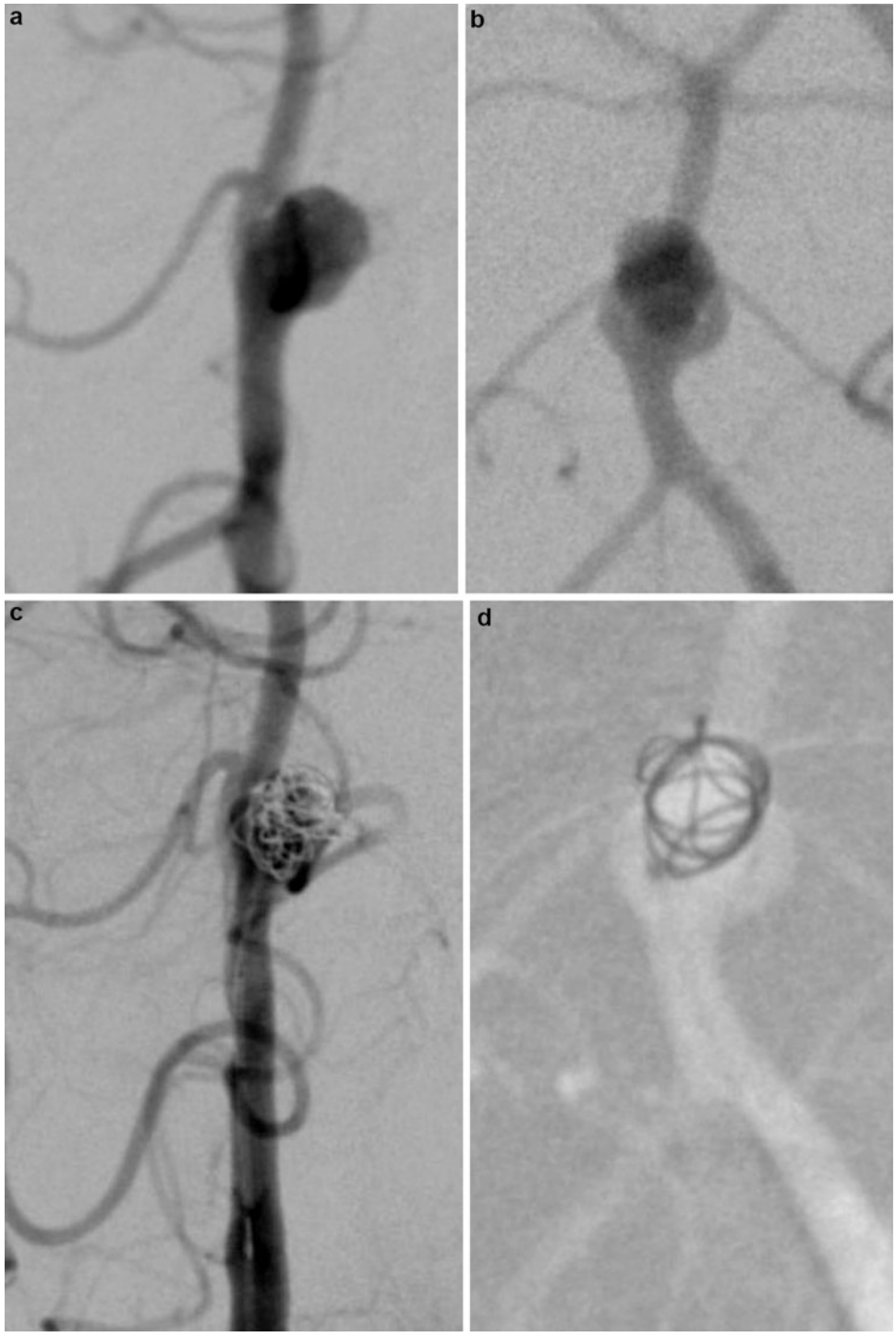

Fig. 2 (continued)

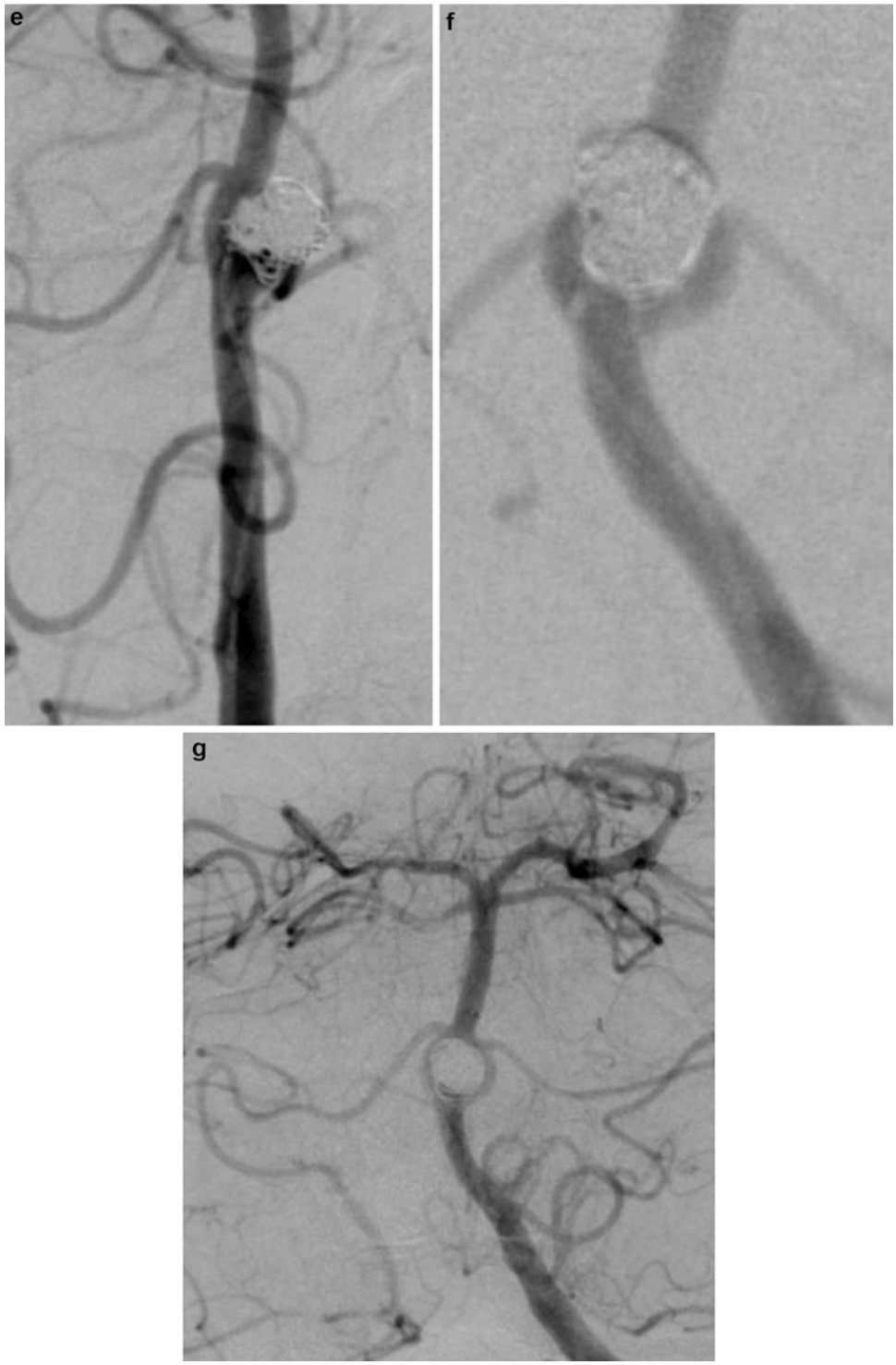

Fig. 2 Endovascular coil occlusion of a ruptured BA trunk aneurysm with associated fenestration of the said artery. The steps of the treatment are shown: selection of a working projections (**a**, **b**), deployment of the framing coil (**c**, **d**), and eventually complete filling of the aneurysm (**e**, **f**) and the final DSA run (**g**)

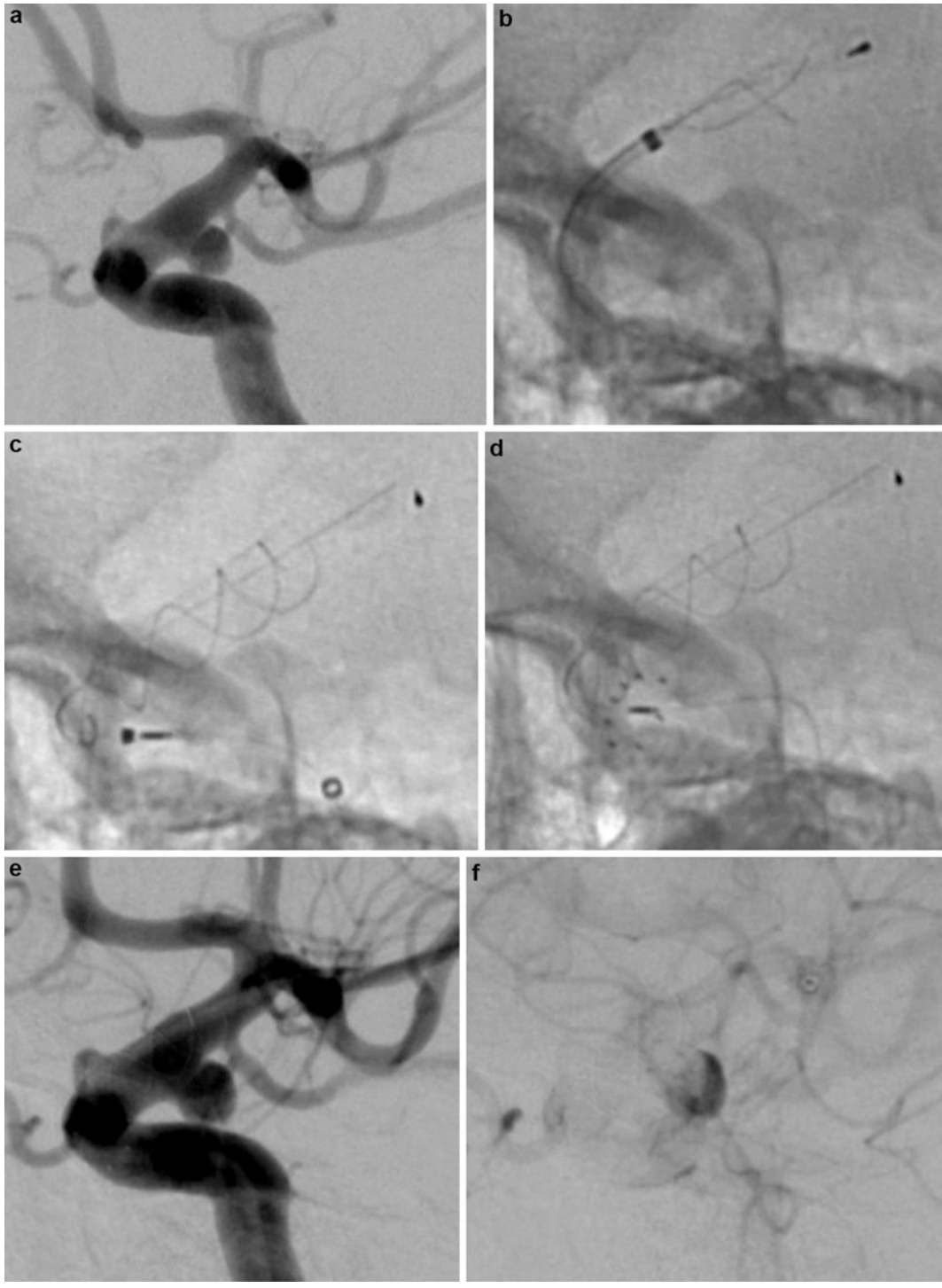

Fig. 3 Endovascular treatment of a left ICA/PcomA aneurysm with a flow diverter stent (p64). The steps of the treatment are shown: selection of a working projection (**a**), well controlled but rapid deployment of the p64 (**b**), full deployment of the p64 prior to mechanical detachment (**c**), complete expansion of the p64 after the mechanical detachment (**d**; note the symmetric, circular distribution of the eight proximal markers). The arterial phase of the final DSA run shows the FDS in place, not covering the PcomA origin (**e**). Late capillary phase of the final DSA run (**f**, note the contrast stagnation within the aneurysm)

segment of the ICA, completely covering the orifice of the said aneurysm. The FDS was then mechanically detached (Fig. 3).

Duration: 1st–10th DSA run: 20 min; fluoroscopy time: 14 min

Complications: none

Post medication: 1× 100 mg ASA PO daily for life, 1× 75 mg clopidogrel PO daily for 1 year

Clinical Outcome

The postprocedural course was uneventful, and the patient was discharged home 12 days after the hemorrhage with no neurological or cognitive deficit (modified Rankin Scale 0, Glasgow Outcome Score 5).

Follow-Up and Subsequent Treatment

The first angiographic follow-up was performed 5 months after the treatment and showed complete occlusion of the BA trunk aneurysm. The ICA/PcomA aneurysm, however, persisted due to a shortening of the p64 resulting in incomplete coverage of the aneurysm neck. We decided to deploy a second FDS distal to the first one in a telescopic fashion. The procedure was performed as for the first FDS implantation and was completed with no periprocedural complications. The second angiographic follow-up was carried out 6 months after the second treatment and showed complete obliteration of the ICA aneurysm and persistent complete occlusion of the BA trunk aneurysm (Fig. 4).

Discussion

This case is an example of a ruptured aneurysm originating from a segmental non-fusion of the basilar artery trunk. Similar examples of ruptured aneurysms at a non-fused segment of the basilar artery trunk are shown below (Figs. 5, 6, and 7).

Normal variants and anomalies of the cerebral vasculature are frequent (Van Den Bergh and Van Der Eecken 1968; Puchades-Orts et al. 1976). Some of these variants are very common and readily apparent on imaging; others, however, are less frequent and require special attention to identify. Both normal variants and anomalies can be associated with an increased frequency to aneurysm formation and rupture.

Some of anatomic variants of the cerebral vasculature are best understood based on the embryonic development of the cerebral vessels. The anterior and posterior cerebral circulation develops separately and differently during embryonic life. While the internal carotid arteries and their branches are formed through serial changes to the pharyngeal arches connecting the ventral and dorsal aortae, the posterior circulation develops from longitudinal anastomoses between the cervical segmental arteries known as the longitudinal neural system. The basilar artery is formed through midline fusion of the posterior longitudinal system. Incomplete fusion to some extent leads to a fenestration or segmental non-fusion of the basilar artery (Padget 1948). Another possible explanation for duplicated segments of the vertebrobasilar system is persistence of the primitive lateral basilovertebral anastomosis (Gregg and Gailloud 2017). The basilar artery and the vertebral arteries are common locations for intracranial arterial fenestration (Sanders et al. 1993). One review of 2280 cranial MR angiographies detected fenestration of the basilar artery in 23 (1%) cases with the majority of detected fenestrations occurring proximal to the origin of the AICA (Tanaka et al. 2006). The incidence of BA fenestration is even higher in postmortem series (Wollschlaeger et al. 1967). Double and multiple concurrent fenestrations of the vertebrobasilar system have also been reported (Fujimura et al. 1997; Stark et al. 2013).

Intracranial arterial fenestration is reported to be associated with higher incidence of intracranial aneurysms of over 30% (Miyazaki et al. 1981; Campos et al. 1987; Picard et al. 1993; Tasker and Byrne 1997; Tanaka et al. 2006). A series of 103 posterior circulation aneurysms reported fenestration of the basilar artery in nine cases, and the aneurysm was located at the site of fenestration in 6 of them (Tasker and Byrne 1997). Possible explanation of the high frequency of aneurysms

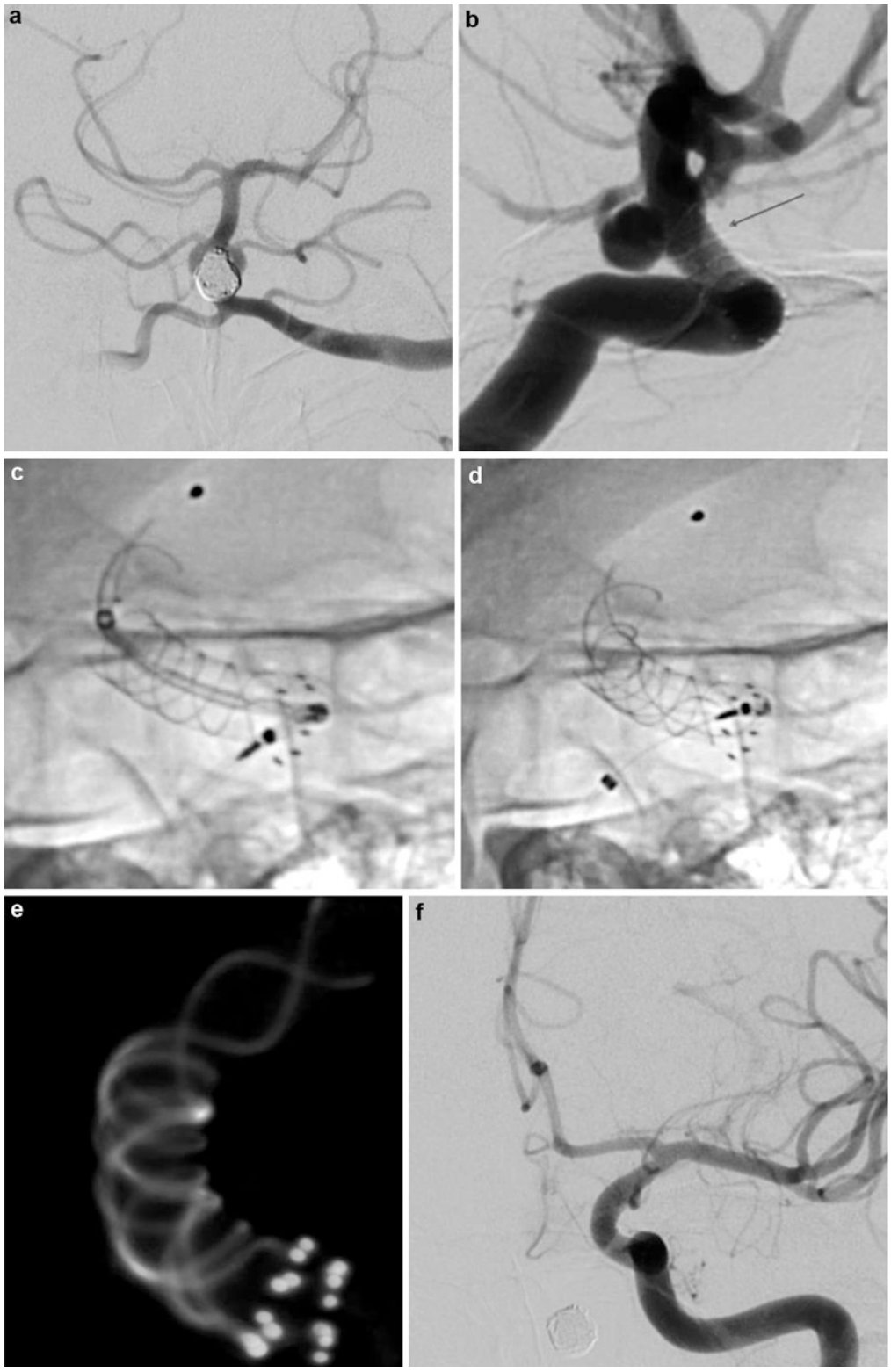

Fig. 4 (continued)

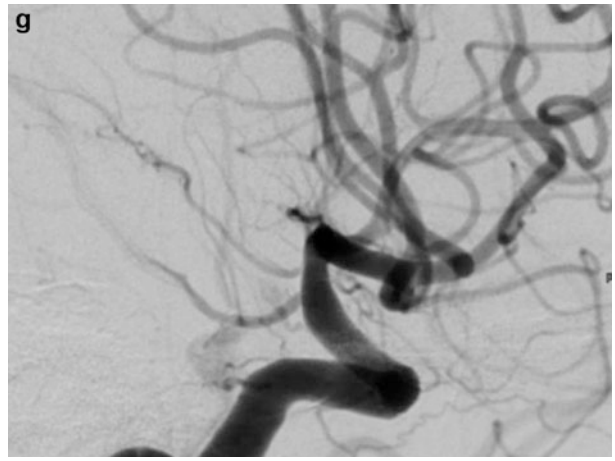

Fig. 4 First angiographic follow-up 5 months after SAH and endovascular aneurysm treatment showing complete occlusion of the BA trunk aneurysm (**a**) and persistent filling of the left ICA/PcomA aneurysm (**b**). Note the foreshortening of the distal end of the FDS (arrow in **b**), which resulted in the aneurysm neck being incompletely covered. Retreatment of the left ICA/PcomA aneurysm with telescopic placement of a second FDS. An Excelsior-XT-27 microcatheter was navigated through the first FDS (**c**). A second p64 was deployed inside the shortened FDS (**d**). Volume-rendered reconstruction of a DynaCT examination showing the two partially overlapping FDS, with the second p64 reaching further distal than the earlier implanted device (**e**). The follow-up DSA 6 months later (posterior-anterior view (**f**), lateral view (**g**)) shows complete exclusion of the ICA/PcomA aneurysm and no in-stent stenosis. The PcomA, despite being covered by the second p64, remained patent

associated with arterial fenestration is defects in the medial layers at the proximal and distal edges of the fenestration (Finlay and Canham 1994). Hemodynamic stress from two separate inflows from both vertebral arteries has been suggested as a possible explanation for the formation of kissing aneurysms at the site of fenestration (Tsuei et al. 2009).

Like the majority of posterior circulation aneurysms, these lesions are frequently best treated via an endovascular approach. Simple coil occlusion can be safely performed if the anatomy is favorable (Nakstad et al. 1998). In the case of a wide-necked aneurysm, an adjunctive device may become necessary (Stark et al. 2013).

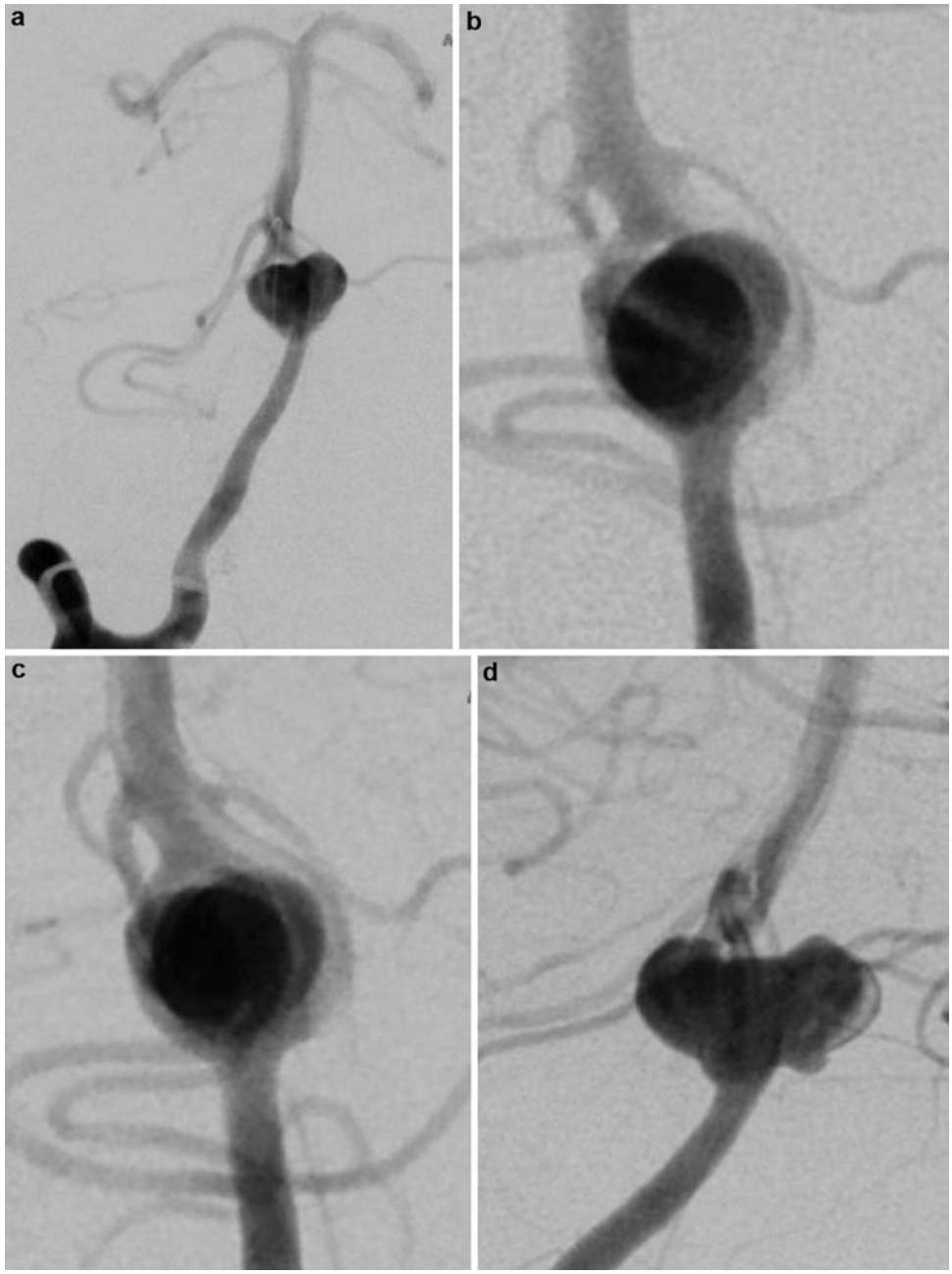

Fig. 5 (continued)

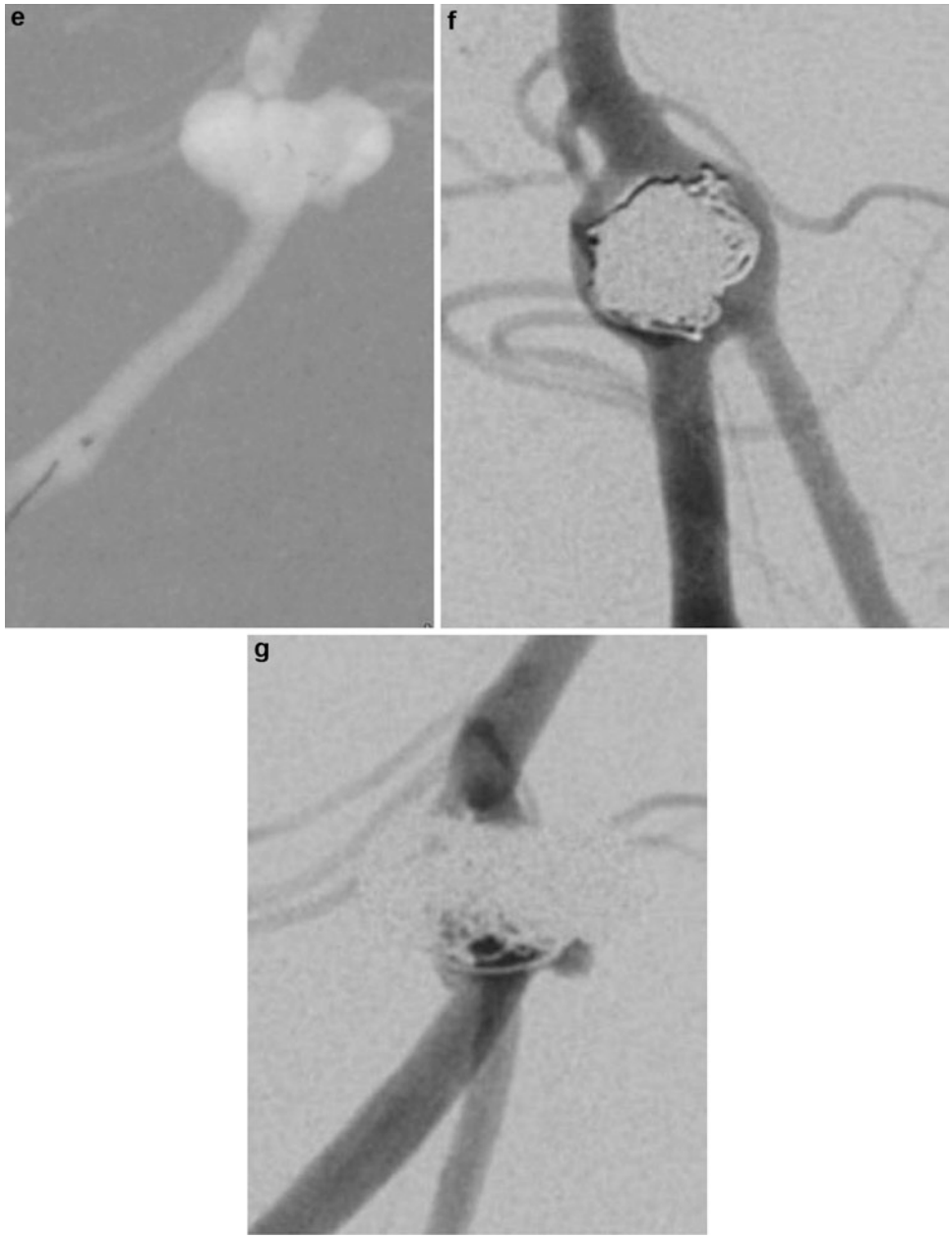

Fig. 5 This 55-year-old woman was admitted due to a diffuse subarachnoid hemorrhage in the basal cisterns and a clot in the fourth ventricle. The angiographic study revealed a heart-shaped aneurysm of the proximal basilar artery with segmental non-fusion proximal to the origin of the AICA (posterior-anterior projection (**a**), 45° RAO (**b**), 45° LAO (**c**)). The aneurysm was treated by stent-assisted coiling using a bifurcation implant (pCONUS, phenox) due to the wide neck of the aneurysm and the lobulated fundus (working projection (**d**), deployment of the pCONUS bifurcation stent (**e**)). The final angiographic runs (**f**, **g**) showed complete occlusion of the aneurysm. Unfortunately the patient developed severe multiple organ failure during the hospitalization and died 19 days after the SAH

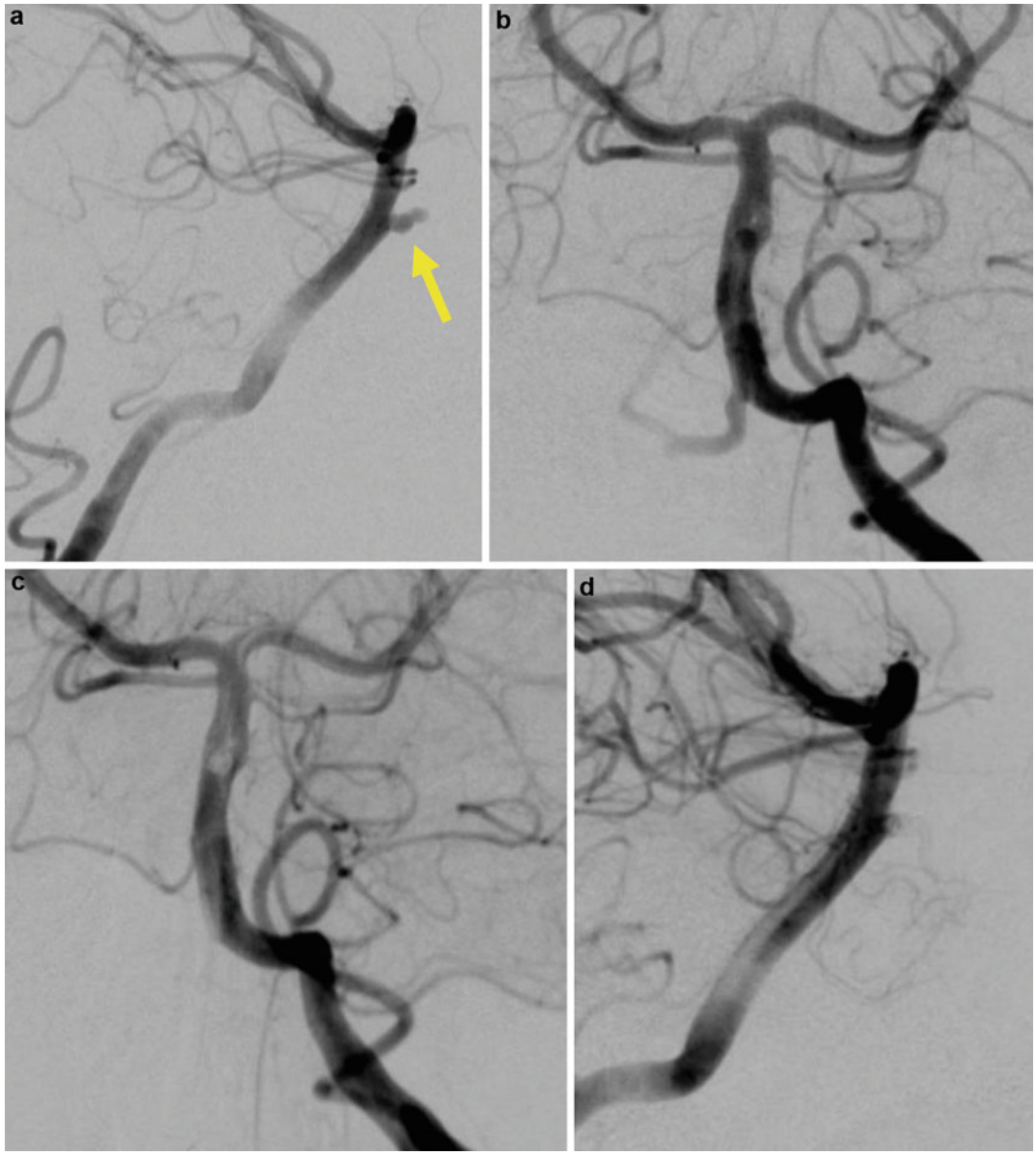

Fig. 6 (continued)

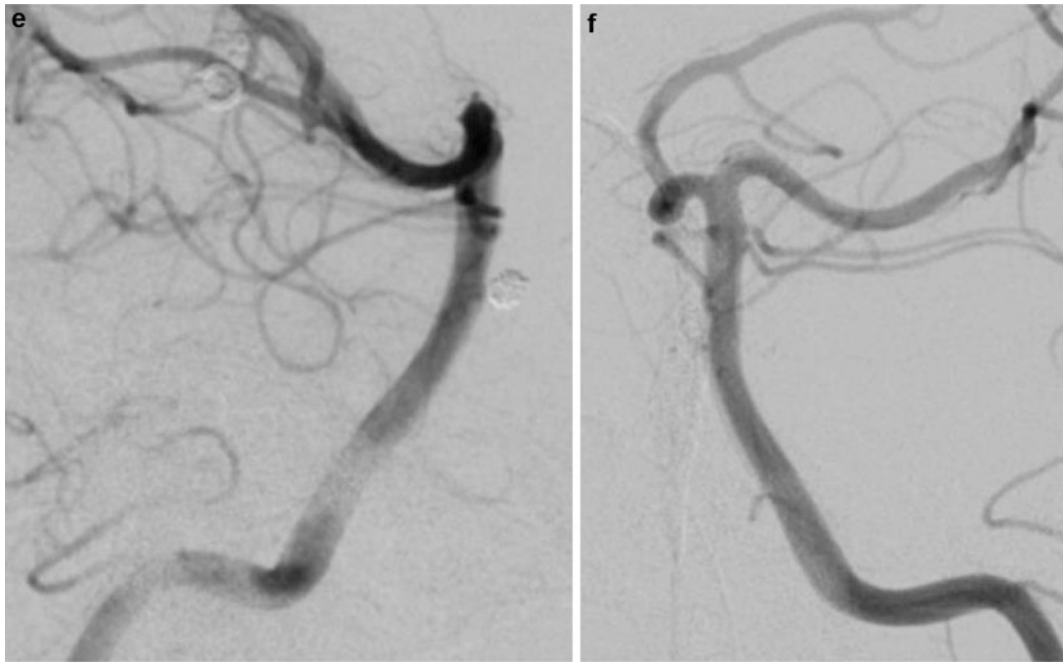

Fig. 6 This 44-year-old female patient presented with an SAH of Hunt and Hess grade IV due to the rupture of a small aneurysm originating from a fenestration of the basilar artery trunk in its middle third (arrow (**a**, **b**)). The aneurysm was partially occluded using a small coil (**c**, **d**). The patient developed severe vasospasm and required prolonged continuous intra-arterial infusion of calcium channel blockers over indwelling microcatheters in both the internal carotid artery and in the left vertebral artery. The patient recovered well. She has remained asymptomatic during 5 years of clinical and angiographic follow-up with permanent occlusion of the aneurysm (**e**, **f**)

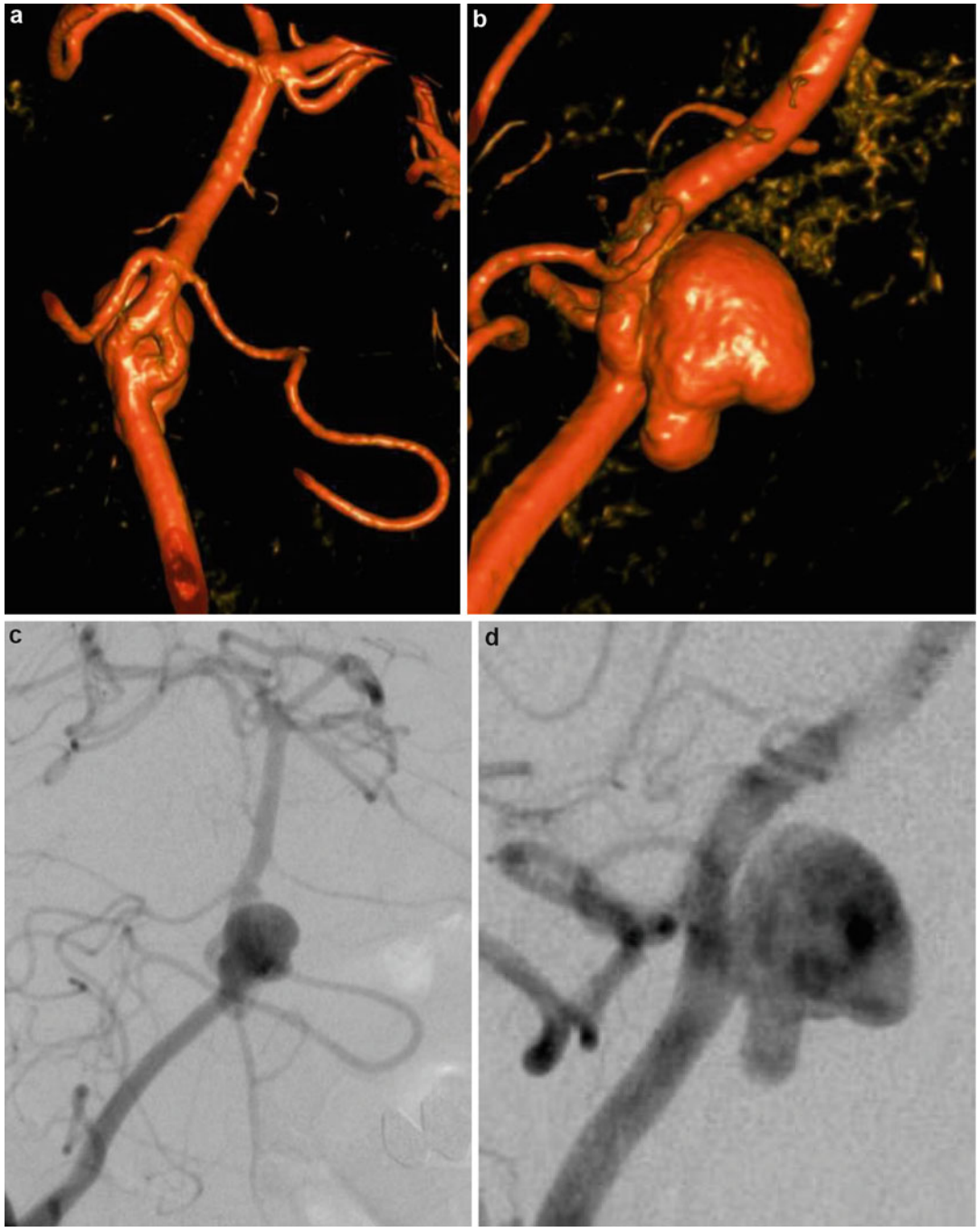

Fig. 7 (continued)

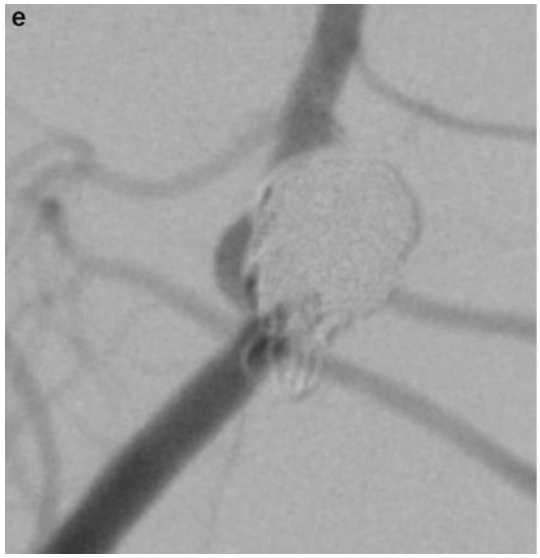

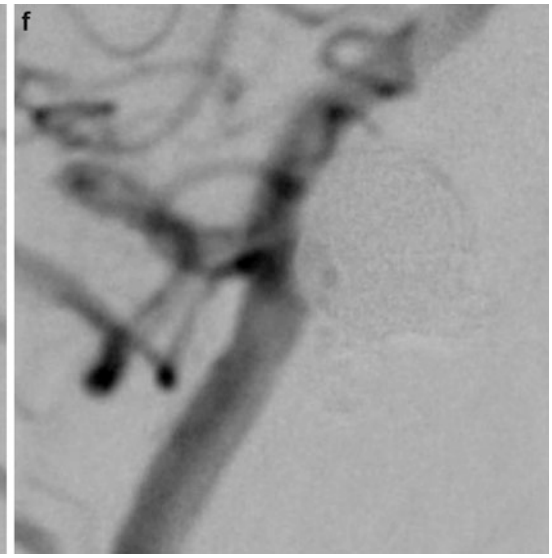

Fig. 7 This 36-year-old female patient experienced a severe and persistent headache after coughing. NCCT revealed a moderate SAH mainly in the prepontine cistern. The cerebral angiography showed a large aneurysm arising at the fenestration of the proximal third of the basilar artery (volume-rendered reconstructions from a rotational angiography (**a**, **b**), posterior-anterior and lateral projections (**c**, **d**)). The aneurysm was treated by complete coil occlusion (**e**, **f**). The patient recovered well from the SAH. Follow-up DSA is pending

Therapeutic Alternatives

Flow Diversion
Stent-Assisted Coiling
WEB

References

Campos J, Fox AJ, Viñuela F, Lylyk P, Ferguson GG, Drake CG, Peerless SJ. Saccular aneurysms in basilar artery fenestration. AJNR Am J Neuroradiol. 1987;8 (2):233–6.

Finlay HM, Canham PB. The layered fabric of cerebral artery fenestrations. Stroke. 1994;25(9):1799–806.

Fujimura M, Sugawara T, Higuchi H, Oku T, Seki H. A ruptured aneurysm at the distal end of the basilar artery fenestration associated with multiple fenestrations of the vertebrobasilar system: case report. Surg Neurol. 1997;47(5):469–72.

Gregg L, Gailloud P. The role of the primitive lateral basilovertebral anastomosis of Padget in variations of the vertebrobasilar arterial system. Anat Rec (Hoboken). 2017;300(11):2025–38. https://doi.org/10.1002/ar.23633.

Miyazaki S, Kamata K, Yamaura A. Multiple aneurysms of the vertebrobasilar system associated with fenestration of the vertebral artery. Surg Neurol. 1981;15(3):192–5. https://doi.org/10.1016/0090-3019(81)90140-3.

Nakstad PH, Bakke SJ, Dale LG, Moen G. Basilar artery fenestration aneurysms treated with guglielmi detachable coils. Interv Neuroradiol. 1998;4(1):75–80. https://doi.org/10.1177/159101999800400109.

Padget DH. The development of the cranial arteries in the human embryo. Contrib Embryol. 1948;32:205–61.

Picard L, Roy D, Bracard S, Per A, Marchal JC. Aneurysm associated with a fenestrated basilar artery: report of two cases treated by endovascular detachable balloon embolization. AJNR Am J Neuroradiol. 1993;14 (3):591–4.

Puchades-Orts A, Nombela-Gomez M, Ortuño-Pacheco G. Variation in form of circle of Willis: some anatomical and embryological considerations: some considerations on the circle of Willis. Anat Rec. 1976;185 (1):119–23. https://doi.org/10.1002/ar.1091850112.

Sanders WP, Sorek PA, Mehta BA. Fenestration of intracranial arteries with special attention to associated aneurysms and other anomalies. AJNR Am J Neuroradiol. 1993;14(3):675–80.

Stark MM, Skeik N, Delgado Almandoz JE, Crandall BM, Tubman DE. Concurrent basilar artery double fenestration with aneurysm and vertebral artery dissection: case report and literature review of rare cerebrovascular abnormalities. Ann Vasc Surg. 2013;27(4):497. e15–21. https://doi.org/10.1016/j.avsg.2012.06.017.

Tanaka M, Kikuchi Y, Ouchi T. Neuroradiological analysis of 23 cases of basilar artery fenestration based on 2280 cases of MR angiographies. Interv Neuroradiol. 2006;12(Suppl 1):39–44. https://doi.org/10.1177/15910199060120S103.

Tasker AD, Byrne JV. Basilar artery fenestration in association with aneurysms of the posterior cerebral circulation. Neuroradiology. 1997;39(3):185–9. https://doi.org/10.1007/s002340050389.

Tsuei YS, Matsumoto Y, Ohta M, Nakayama T, Ezura M, Takahashi A. Vertebrobasilar junction fenestration with dumbbell-shaped aneurysms formation: computational fluid dynamics analysis. Surg Neurol. 2009;72(Suppl 2):S11–9. https://doi.org/10.1016/j.surneu.2009.05.026.

Van Den Bergh R, Van Der Eecken H. Anatomy and embryology of cerebral circulation. Prog Brain Res. 1968;30:1–25. https://doi.org/10.1016/S0079-6123(08)61433-8. Elsevier.

Wollschlaeger G, Wollschlaeger PB, Lucas FV, Lopez VF. Experience and result with postmortem cerebral angiography performed as routine procedure of the autopsy. Am J Roentgenol Radium Therapy, Nucl Med. 1967;101(1):68–87.